



PERGAMON

Deep-Sea Research I 49 (2002) 1837–1852

DEEP-SEA RESEARCH  
PART I

www.elsevier.com/locate/dsr

# Sulfate reduction and iron sulfide mineral formation in the southern East China Sea continental slope sediment

Saulwood Lin\*, Kuo-Ming Huang, Shin-Kuan Chen

*Institute of Oceanography, National Taiwan University, #1, Roosevelt Road, Section 4, Taipei 106, Taiwan*

Received 5 July 2001; received in revised form 27 March 2002; accepted 23 July 2002

## Abstract

Sulfate reduction rate, organic carbon and sulfide burial rate; organic carbon, carbonate carbon, and reactive iron contents; grain size; and sedimentation rate were determined in sediments of the southern East China Sea continental slope. The results show high sulfate reduction and pyrite sulfur burial rates in slope areas with high organic carbon and sedimentation rates. Unusually high rates of organic carbon deposition enhance sulfate reduction and pyrite sulfide burial in the region.

Both sulfate reduction rates and pyrite sulfur burial rates increased linearly with increasing organic carbon burial rate, indicating that deposition of organic carbon on the slope is the primary controlling factor for pyrite formation. Abundant reactive iron indicated that iron is not limiting pyrite formation. Pyrite is the predominant sulfide mineral; however, acid volatile sulfide constituted up to 50% of total sulfide at some stations. Up to 240  $\mu\text{mol/g}$  of pyrite sulfur and 5  $\text{mmol/m}^2/\text{day}$  of sulfate reduction rates were found in the slope sediment. Sulfate reduction rate and pyrite sulfur did not decrease with increasing overlying water depth.

High organic carbon burial rates enhanced the sulfate reduction rate and subsequently the rate of pyrite sulfur burial in the slope region. As a result, the southern East China Sea continental slope environment is an efficient pyrite sulfur burial environment.

© 2002 Elsevier Science Ltd. All rights reserved.

*Keywords:* Sulfate reduction; Pyrite; Organic carbon; Continental slope; East China Sea; Sedimentation rate

## 1. Introduction

Determination of sulfide burial is important in understanding the fate of organic carbon, since bacterial sulfate reduction is a major pathway for the organic carbon oxidation in marine sediments. Sulfate reduction in anoxic sediments accounts for up to 50% of the organic carbon oxidation

(Jorgensen, 1982; Canfield, 1993). Furthermore, pyrite burial has exerted a major regulation on the atmospheric oxygen level throughout the Phanerozoic (Berner et al., 2000; Berner, 1998; Berner and Canfield, 1989; Lasaga, 1989; Berner, 1987; Garrels and Lerman, 1984; Holland, 1978) and on the Proterozoic ocean chemistry (Canfield, 1998). By modeling of the Phanerozoic atmospheric oxygen level, Berner and Canfield (1989) showed that past atmospheric oxygen level was controlled by the rapid redistribution of sediments between

\*Corresponding author. Tel./fax: +886-2-2363-6424.

E-mail address: swlin@cems.ntu.edu.tw (S. Lin).

the marine clastic, coal basin and other continental clastic sedimentary environments. The understanding of sediment deposition and the associated sulfide and organic carbon burial in various environments, their relative abundance and redistribution, therefore, were key factors in determining the past atmospheric oxygen level.

In the modern ocean, the major sulfide and organic carbon burial takes place at continental margins, in particular in delta and shelf sediments (Berner, 1982). A study of pyrite formation in the Mississippi River Delta, shelf and slope also confirmed that the delta and shelf are the dominating sulfide burial environments in the Gulf of Mexico (Lin and Morse, 1991). Since organic carbon is the primary limiting factor for both sulfate reduction and pyrite formation in most marine environments (Berner, 1970; Raiswell and Berner, 1985), and deltas and shelves receive a great majority of the organic carbon delivered to the marine environment (Berner, 1982), delta and shelf sediments are generally considered as the primary sulfide burial environment in the modern ocean.

Sediments of the slope and deep sea are usually regarded as less important for sulfide formation and burial, since decomposition of organic carbon sinking through the deep water column reduces the organic carbon deposition. The study of sulfate reduction rate in the Gulf of Maine (Christensen, 1989) showed that sulfate reduction decreased rapidly with increasing water depth. However, a limited but growing volume of data (Suits and Arthur, 2000; Ferdelman et al., 1999; Thamdrup and Canfield, 1996; Lein, 1985) on sulfate reduction rates in the slope region shows that significant sulfate reduction rates and pyrite sulfur concentrations do exist in the slope environment. Furthermore, Volkov and Rozanov (1983) showed that the continental slope was an important pyrite burial environment during the Holocene, perhaps twice that in modern shelf sediments.

In order to better understand the oceanic distribution of pyrite burial, this study focused on sulfate reduction and pyrite formation in the southern East China Sea slope region, where relatively high concentrations of organic carbon and high sedimentary fluxes were observed. We

examined the spatial distributions and controlling factors of sulfate reduction and pyrite with respect to water depth and sedimentation rate.

## 2. Methods

### 2.1. Study area

The East China Sea continental margin is one of the largest shelf and slope systems. The western boundary current, the Kuroshio, turns from northward to northeastward flow as it impinges on the southern East China Sea continental margin (Fig. 1). Upwelling is associated with the topographic deflection of a counter-clockwise branch current (Tang et al., 2000; Liu et al., 1992), which continuously pumps high nutrient water to the surface and supports high primary productivity with an annual mean of  $549 \pm 84 \text{ mgC/m}^2/\text{day}$  (Gong et al., 2000). However, most organic carbon is not depositing directly on the outer shelf because of the high current speeds (maximum speed: 100 cm/s) within the Kuroshio in the study area. Outer and middle shelf sediments under the Kuroshio are composed mostly of coarse-grained shell fragments and relict quartz sand from the last glaciation and contain very little organic carbon (Lin et al., 2002, 1992). Most organic particulates and fine-grained sediments are horizontally transported from the middle and outer shelf and deposited in the quiescent slope region (Hung and Chung, 1998; Lin et al., 1992; Narita et al., 1990).

### 2.2. Sampling and sample handling

Sediment samples were collected with a Benthos gravity core or piston core on board the R/V *Ocean Researcher-I*. Most cores were sectioned in 2 cm depth intervals in a nitrogen-filled glove bag (Aldrich) immediately after the sediment arrived on board, with a total sectioning time of <3 h. Subsamples in the air-tight Plexiglas coring tubes were injected with  $1\text{--}2 \mu\text{Ci Na}_2^{35}\text{SO}_4$  (NEN, DuPont) and incubated for 24 hours at  $9^\circ\text{C}$  in the dark. After incubation, samples were kept frozen. A set of subsamples was centrifuged

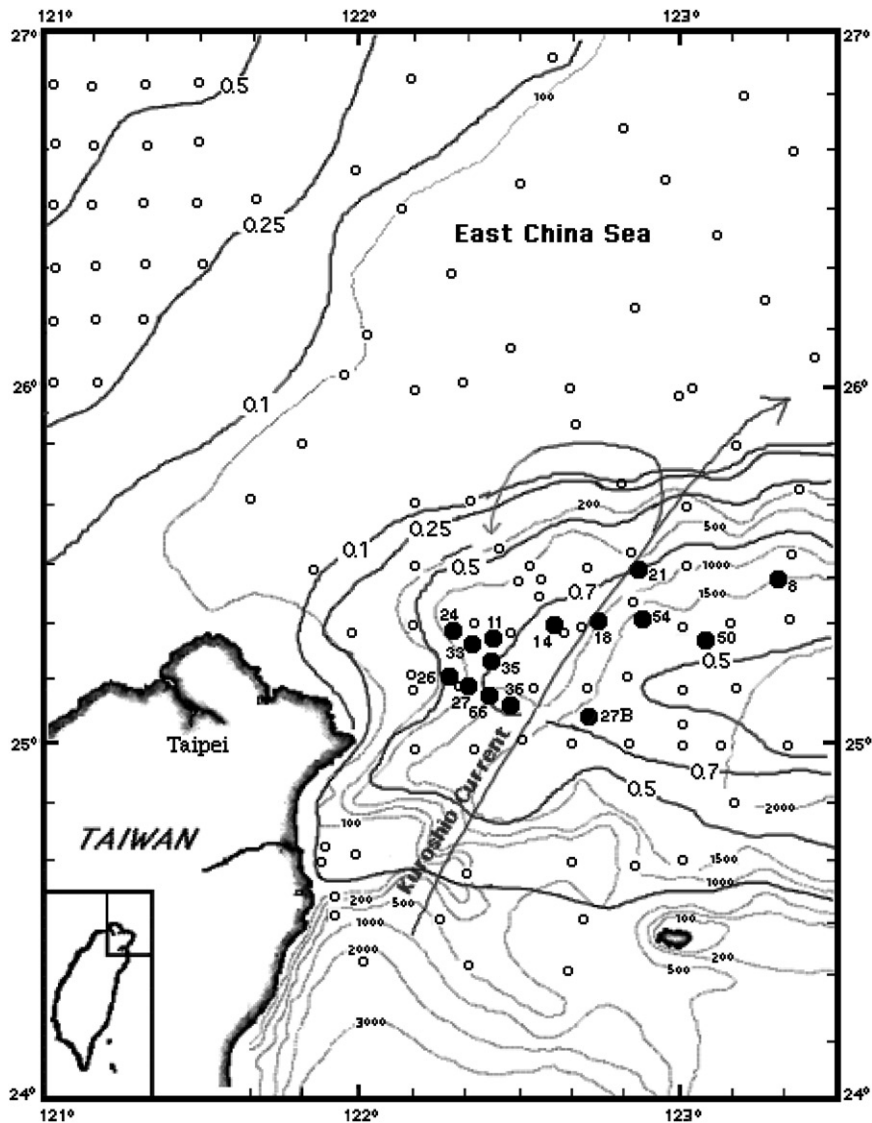


Fig. 1. Sampling stations (●) and % organic carbon distribution (black line) in the study area. Open circles (○) are stations at which only the surface sediment organic carbon concentration was measured. Depth contours are in meters (gray line). Numbers next to the station (●) are station number. Arrow shows the Kuroshio current and branched current flow directions.

(4000 rpm, 15 min) and filtered (Nuclepore, 0.45  $\mu\text{m}$ ) to obtain pore water. Part of the pore water was used for dissolved sulfide analysis on board by the methylene blue method (Cline, 1969). Pore water samples were stored in polyethylene vials at 4°C until sulfate determination in the laboratory. Other subsamples of sediment were

stored frozen in polyethylene centrifuge tubes for AVS and pyrite-S analyses and grain size determinations. After freeze-drying for 1 week in a Labconco freeze-drier, sediments were ground in an agate mortar and stored in polypropylene vials for organic carbon, carbonate, iron, Pb-210, or C-14 determinations.

### 2.3. Grain size

Grain sizes were determined by the pipette method of Folk (1968). Approximately 15 g of wet sediment were placed in a graduated cylinder, stirred, and sampled sequentially. Standard deviations of triplicate analyses were less than 8%.

### 2.4. Porewater sulfate

Pore water sulfate concentrations were determined by ion chromatography (O'Dell et al., 1984) with a Dionex 4500i ion chromatograph equipped with a conductivity detector and an IonPac AS4A anion exchange column. Samples were usually diluted 100-fold prior to analysis. 1.7 mM NaHCO<sub>3</sub> was used as the eluent and 1.8 mM Na<sub>2</sub>CO<sub>3</sub> with 0.025 N H<sub>2</sub>SO<sub>4</sub> as the regeneration fluid. The precision of sulfate analysis was 0.4%.

### 2.5. Organic and carbonate carbon

Total carbon and organic carbon were analyzed with a LECO C/S analyzer (SC-444) equipped with a high temperature resistance furnace and an IR detector. Approximately 0.3 g of dry sediment was combusted at 1400°C with high purity oxygen to determine the total carbon content. Organic carbon was determined with pre-acidified (~2 ml 6N HCl) and hot plate dried (~50°C, 8 h) sediments. Calcium carbonate content (wt%) was calculated from the difference between total carbon and organic carbon assuming that calcite was the only carbonate phase. The precision for the total carbon and organic carbon was 1.2% and 3%, respectively.

### 2.6. Sulfate reduction rate

Sulfate reduction rates were measured by the <sup>35</sup>SO<sub>4</sub> technique (Jorgensen, 1978; Lin and Morse, 1991; Lin et al., 2000). Incubated sediments were distilled in an oxygen-free vessel for 1 h to extract the reduced <sup>35</sup>S. The H<sub>2</sub> <sup>35</sup>S evolved from boiling Cr(II)+acid distillation was carried into a Zn-acetate (0.28 M) trap with high purity nitrogen (99.9%). The radioactivity of Zn<sup>35</sup>S and the

remaining <sup>35</sup>SO<sub>4</sub> were analyzed with a liquid scintillation counter (Packard 1600TR).

### 2.7. Pyrite-S and AVS

Pyrite-sulfur was determined by the Cr(II)+6 N HCl extraction method, and AVS (acid volatile sulfide) was measured by the cold 6 N HCl extraction technique (Cornwell and Morse, 1987; Canfield et al., 1986).

### 2.8. Oxalate extractable iron and total iron

Iron was extracted with buffered 0.2 M ammonium oxalate + 0.1 M oxalic acid for 4 h. For total iron, sediment was digested in a CEM microwave digestion system (MDS-2000) with 2.5 ml of HNO<sub>3</sub>: HF (5:2) and 10 ml of 4% H<sub>3</sub>BO<sub>3</sub> mixture (Lin et al., 2002). After the extraction, iron was determined with an atomic absorption spectrometer (Perkin-Elmer 3300). The total iron recovery based on NIST 1646 standard sediments was 101 ± 2% (n = 15).

### 2.9. Pb-210 and C-14

Sedimentation rates were measured by the Pb-210 method through alpha counting of its daughter Po-210 (Flynn, 1968; Shokes, 1976; Nittrouer et al., 1979; Smith and Hamilton, 1984). A Po-209 spike (Isotope Products Lab, CA) was added to approximately 5 g of dry sediment prior to leaching with concentrated HNO<sub>3</sub>. The extracted solution was filtered, evaporated, and re-dissolved in HCl. After the pH was adjusted to ~1.5 with NH<sub>4</sub>OH, Po isotopes were plated on a silver planchet (1", United Mineral, NY). Polonium radioactivities were determined with EG&G Ortec silicon surface barrier detectors connected to a Seiko EG&G Multichannel analyzer (7800). Counting errors were usually < 5%.

Sediment organic carbon C-14 was analyzed by accelerator mass spectrometry by the Rafter Radiocarbon Laboratory, New Zealand. Age determinations followed Stuiver and Polach (1977).

### 3. Results

#### 3.1. Organic carbon

Organic carbon concentrations decreased seawards from the inner shelf (mean:  $0.43 \pm 0.094\%$ ) to the outer shelf (mean:  $0.036 \pm 0.047\%$ ) (Fig. 1). Very little organic carbon was found in the middle and outer shelf sediments, which were composed of coarse-grained quartz sand and carbonate shells. From the outer shelf, organic carbon concentrations increased with increasing water depth. The highest concentration ( $\sim 0.8\%$ ) was observed in the upper slope sediments (approximately 800–1500 m water depth). At greater depth, its concentration decreased to  $\sim 0.5\%$ .

The spatial distribution of organic carbon was related to the sediment grain size (Fig. 2). Organic carbon concentrations increased with increasing fine-grained sediments (diameter  $< 64 \mu\text{m}$ ). The predominant grain size from inner shelf to slope gradually shifted from sandy silt (inner shelf, mean silt% =  $48.4 \pm 14.8\%$ ), sand (outer shelf, mean sand% =  $92.4 \pm 4.99\%$ ), to silty clay (slope, mean clay% =  $41.9 \pm 19.5\%$ ). Organic carbon concentrations were very low in the outer shelf

sediments even though the water column primary productivity is as high as  $1537 \text{ mgC/m}^2/\text{day}$  (Shiah et al., 1995). Evidently, most fine-grained sediments with higher concentrations of organic carbon were deposited on the upper slope. Hung and Chung (1998), Lin et al. (1992) and Narita et al. (1990) showed that organic carbon associated with fine-grained particles is transported laterally and re-deposited on the slope.

In addition to the grain-size, the carbonate content also affected the organic carbon concentration. Two types of organic carbon vertical profiles were observed (Fig. 3): one showed little variation with depth (e.g. Station 366-35) and the other a decrease with depth (e.g. Station 356-8). The carbonate contents displayed a mirror image distribution as compared to the organic carbon profiles (e.g. Station 366-26, 366-27, 366-35).

#### 3.2. Carbonate

The total carbonate content (wt%) varied greatly, from 3.7% to 87%. The average carbonate concentration increased from the inner shelf (mean:  $7.98 \pm 1.46\%$ ) to the outer shelf (mean:

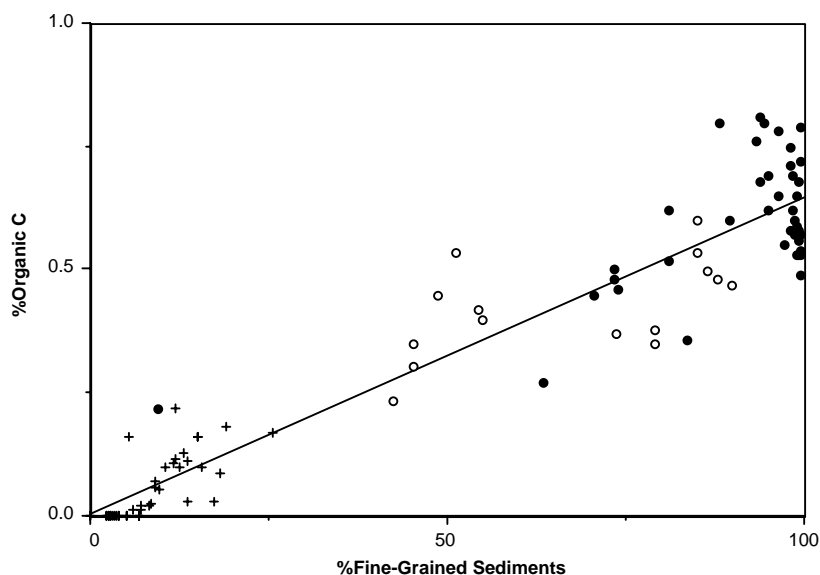


Fig. 2. Organic carbon concentration of the surface sediments increased linearly with increasing percentage of fine-grained sediments. (○): inner shelf, (+): outer shelf, (●): slope sediments.

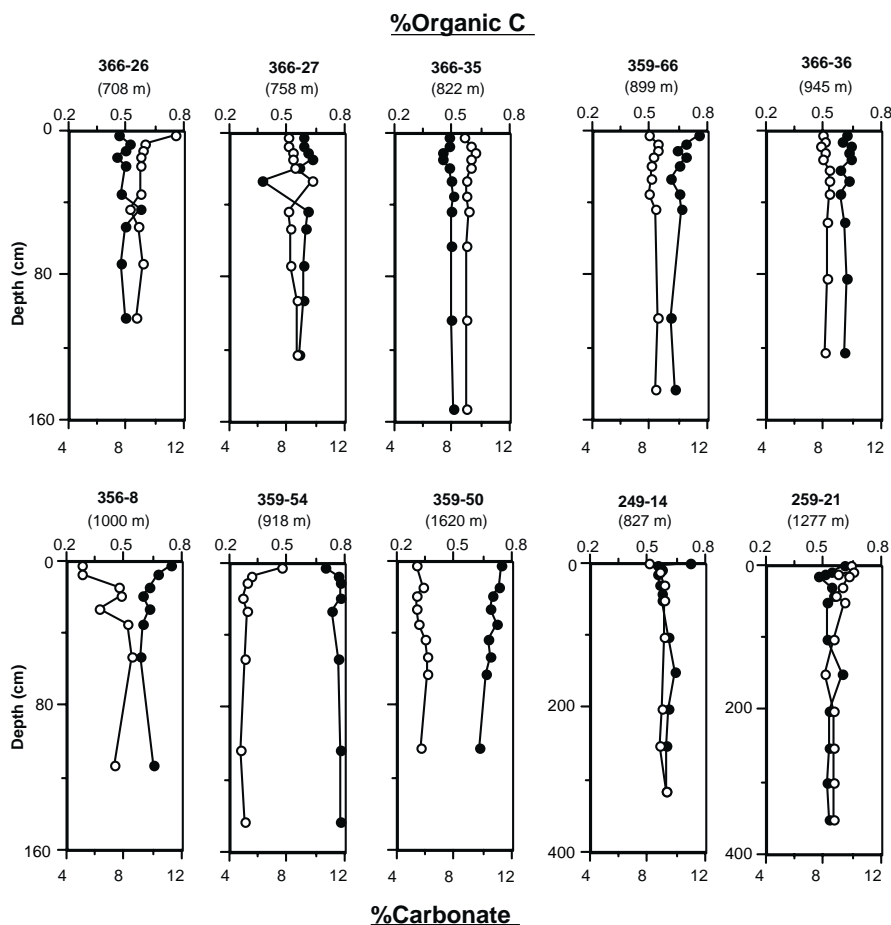


Fig. 3. Organic carbon (●) and carbonate content (○) variations with depth. Numbers in parentheses are overlying water depth at each station.

$23.4 \pm 19.1\%$ ). The highest concentrations (up to 87%) were observed in sediments near the shelf break, where the Kuroshio impinges on the shelf. Calcareous shell debris and coarse-grained quartz sand were the principle components of the outer shelf sediments, which contained very little fine-grained aluminosilicate sediments. Down-slope from the shelf break, the carbonate content decreased rapidly with an overall mean of  $7.87 \pm 1.20\%$  in the slope sediments, similar to that in the inner shelf sediments. The average carbonate contents (%) in most cores were about 8% with some (e.g. Station 359-54 and 50) having a low value of  $\sim 5.5\%$  (Fig. 3).

### 3.3. Porewater sulfate

Porewater sulfate concentrations showed clear evidence of sulfate depletion with depth in the slope sediments (Fig. 4). In upper slope sediments (Stations 26, 66), they decreased from a surface value of  $\sim 29$  mM to 19 mM at about 120 cm. At Stations 35 and 36, concentrations in the surface sediments were only 25 mM, probably a result of rapid sulfate reduction near the sediment surface (see discussion on sulfate reduction rates below). At depth, sulfate decreased rapidly to about 8 mM at 40 cm (Station 36) and 11 mM at 120 cm (Station 35). At Stations 50 and 8, sulfate

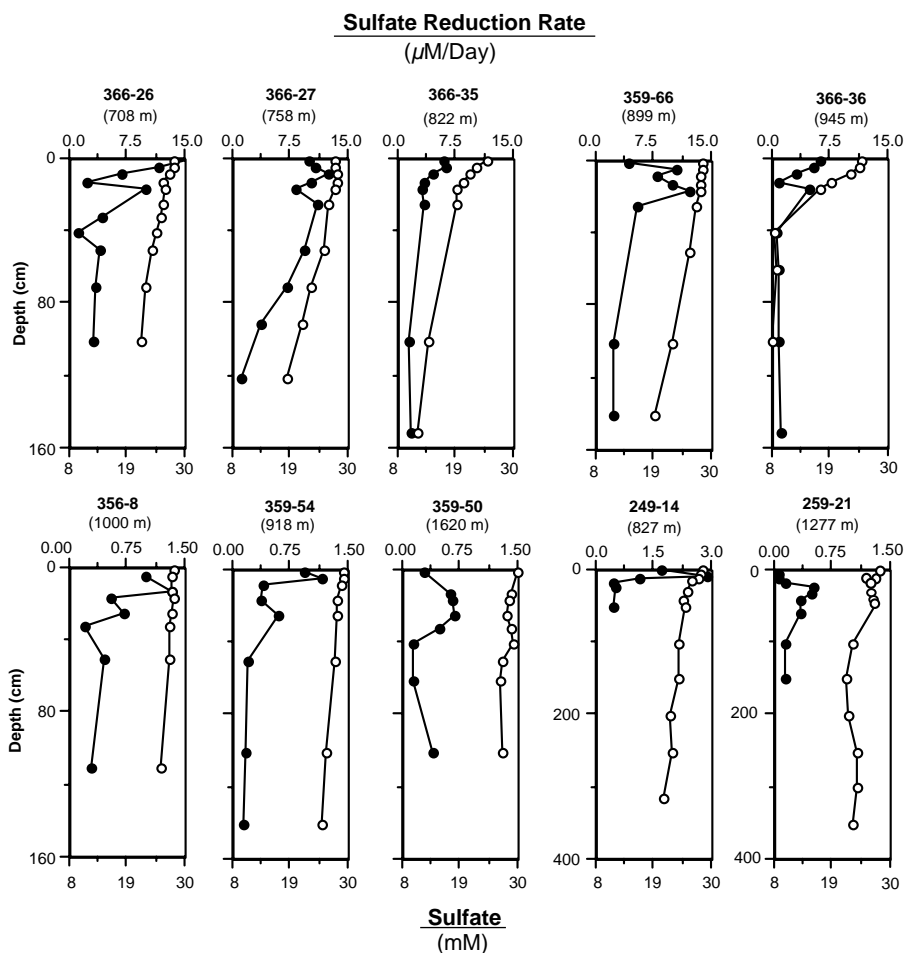


Fig. 4. Sulfate reduction rate (●) and sulfate concentration (○) variations with depth. Notice the scale change for the sulfate reduction rates.

decreased from  $\sim 29$  to  $26$  mM at depth. At Station 249-14, sulfate depletion was observed even down to  $300$  cm.

### 3.4. Sulfate reduction rates

Sulfate reduction rates varied from  $0.1$  to  $15$   $\mu\text{M}/\text{day}$  (Fig. 4). The depth where the maximum rate ( $0.5$ – $15$   $\mu\text{M}/\text{day}$ ) occurred varied from the sediment/water interface to about  $25$  cm. Sulfate reduction rates generally decreased from the rate maximum with increasing depth in the sediment.

### 3.5. Pyrite-S and AVS

Pyrite was the predominant sulfide mineral in the study area; AVS (acid volatile sulfide), however, constituted up to  $50\%$  of the total reduced S at depth (Station 366-36, Fig. 5). Pyrite-S concentrations were in the range  $0$ – $240$   $\mu\text{mol}/\text{g}$  and AVS  $0$ – $25$   $\mu\text{mol}/\text{g}$ . AVS gradually increased and then leveled off at depth. AVS concentrations were comparable to those observed in Peruvian slope sediment (Suits and Arthur, 2000). No dissolved sulfide was found in the pore water within the study area, probably as a result of abundant

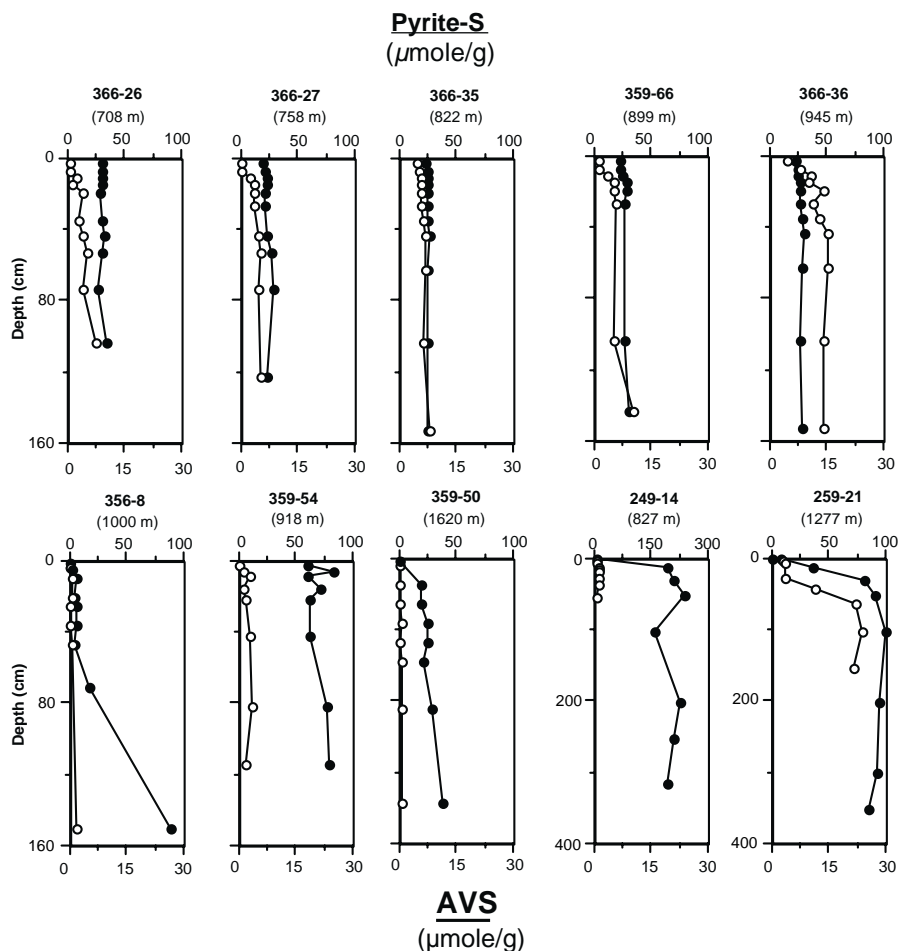


Fig. 5. Pyrite-sulfur (●) and AVS-sulfur (○) concentration profiles. Notice the scale change for the Station 249-14.

reactive iron in the sediments (see discussion below).

Pyrite-S displayed either little variation or an increase with depth. A pyrite-S concentration of ca.  $25 \mu\text{mol/g}$  was observed in sediments with high sulfate reduction rates (e.g. Stations 366-26, 27, 35, 36, 359-66). The concentration was near zero in the surface sediments at stations with lower sulfate reduction rate and then increased with increasing depth (e.g. Station 50, 249-14, 259-21). Pyrite formation did not appear to reach its maximum level within the sampling depth at some stations (e.g. 356-8). The highest pyrite-S concentration ( $\sim 240 \mu\text{mol/g}$ ) of the slope region, observed at Station 249-14 with relatively low sulfate reduction

rates, even exceeded that in the continental shelf sediments.

### 3.6. Oxalate extractable iron and total iron

The concentrations of oxalate extractable iron (reactive iron) and total iron were  $50\text{--}120 \mu\text{mol/g}$  and  $500\text{--}800 \mu\text{mol/g}$ , respectively (Fig. 6). Two patterns of iron concentrations were observed: (A) low concentrations of reactive iron (mean:  $85.6 \pm 15.6 \mu\text{mol/g}$ ,  $11.8 \pm 2.4\%$  of the total) but high total iron (mean:  $755 \pm 48.1 \mu\text{mol/g}$ ) (Station 356-8, 359-50, 54, 249-14, 259-21) and, (B) high concentrations of reactive iron (mean:  $110 \pm 4.15 \mu\text{mol/g}$ ,  $18.4 \pm 0.8\%$  of the total) and low

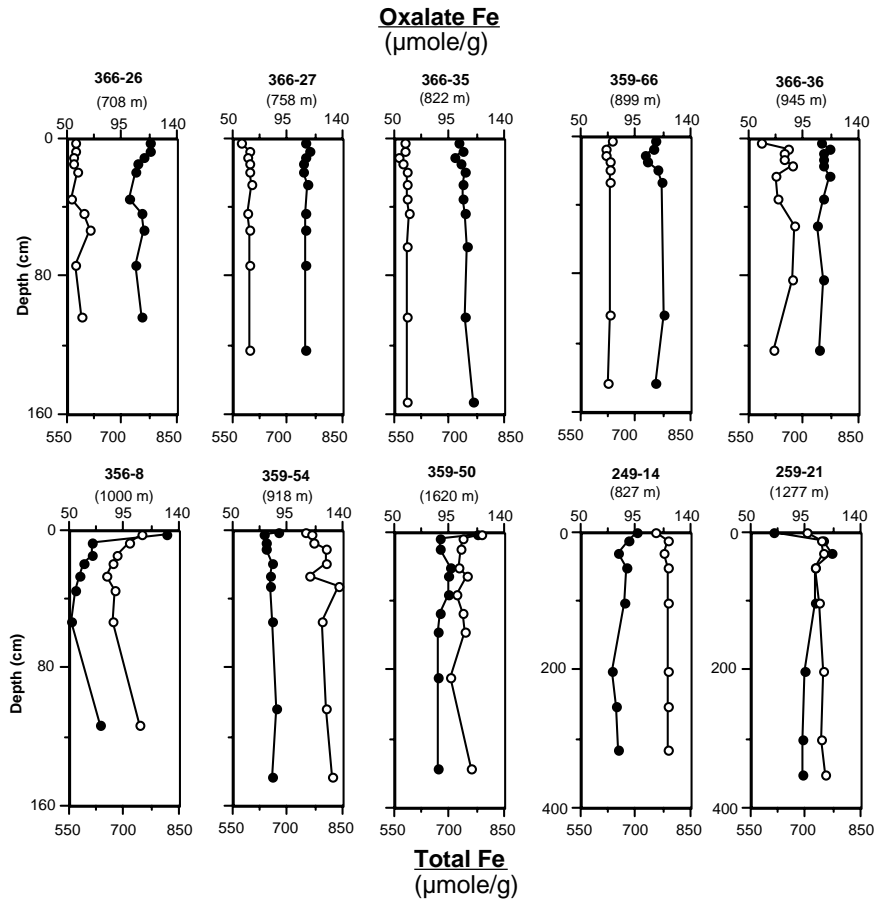


Fig. 6. Oxalate extractable iron (●) and total iron (○) vs. depth. Notice the scale difference for the total and extractable iron.

total iron (mean:  $602 \pm 30.2 \mu\text{mol/g}$ ) (Station 366-26, 27, 35, 36, 359-66). The A-type sediments had higher concentrations of pyrite than the B-type. High concentrations of reactive iron indicate that iron is unlikely to limit pyrite formation.

Concentrations of oxalate iron, in general, were higher than in Long Island Sound sediments but lower than in Mississippi River Delta sediments (Canfield, 1989b). Oxalate and total iron concentrations resembled those in the East China Sea continental shelf sediments (Huang and Lin, 1995).

### 3.7. Sedimentation rates

Sedimentation rates determinations were based on the assumed steady-state distribution of Pb-210

in sediments

$$\frac{dA}{dt} = D \frac{d^2A}{dz^2} - \omega \frac{dA}{dz} - \lambda_{\text{Pb}} A = 0, \quad (1)$$

where  $A$  is the activity of Pb-210;  $t$  the time;  $D$  the particle mixing coefficient;  $\omega$  the sedimentation rate; and  $\lambda_{\text{Pb}}$  the decay constant of Pb-210. If mixing is insignificant, then Eq. (1) reduces to

$$-\omega \frac{dA}{dz} - \lambda_{\text{Pb}} A = 0, \quad (2)$$

which has the solution

$$A(z) = A_0 \exp[-(1/\omega)z], \quad (3)$$

where  $A(z)$  is the activity of Pb-210 at depth  $z$  and  $A_0$  is the initial activity. The apparent sedimentation rates were calculated for each core by

applying Eq. (3) to the log-linear portion of the excess Pb-210 distributions (Fig. 7). Since no apparent sediment mixing was observed near the top of any of the cores (e.g. Station 359-66) with 2 cm sampling interval, all data were used in the sedimentation rate calculation.

The apparent sedimentation rates varied from 0.1 to 0.87 cm/year (Fig. 7). The sedimentation rates of this study were very similar to those measured by Chung and Chang (1995), 0.1–0.57 cm/year, in the same study area. Supported Pb-210 was in a narrow range of 1.18–1.72 dpm/g, also similar to values measured by Chung and Chang (1995). Sedimentation rates in the slope

region were unusually high. Chung and Chang (1995) indicated that a higher Pb-210 flux was a result of either boundary scavenging or lateral transport of the fine-grained sediments from the adjacent shelf.

High sedimentation rates were observed mostly in the region west of the Kuroshio, whereas sedimentation rates were low in the region underneath and east of the Kuroshio. Sedimentation rates could not be determined by the Pb-210 method at a number of stations where excess Pb-210 was observed only in the surface sediments (e.g. Station 249-14, 259-21, Fig. 7). Total Pb-210 in surface sediments of these stations were in the

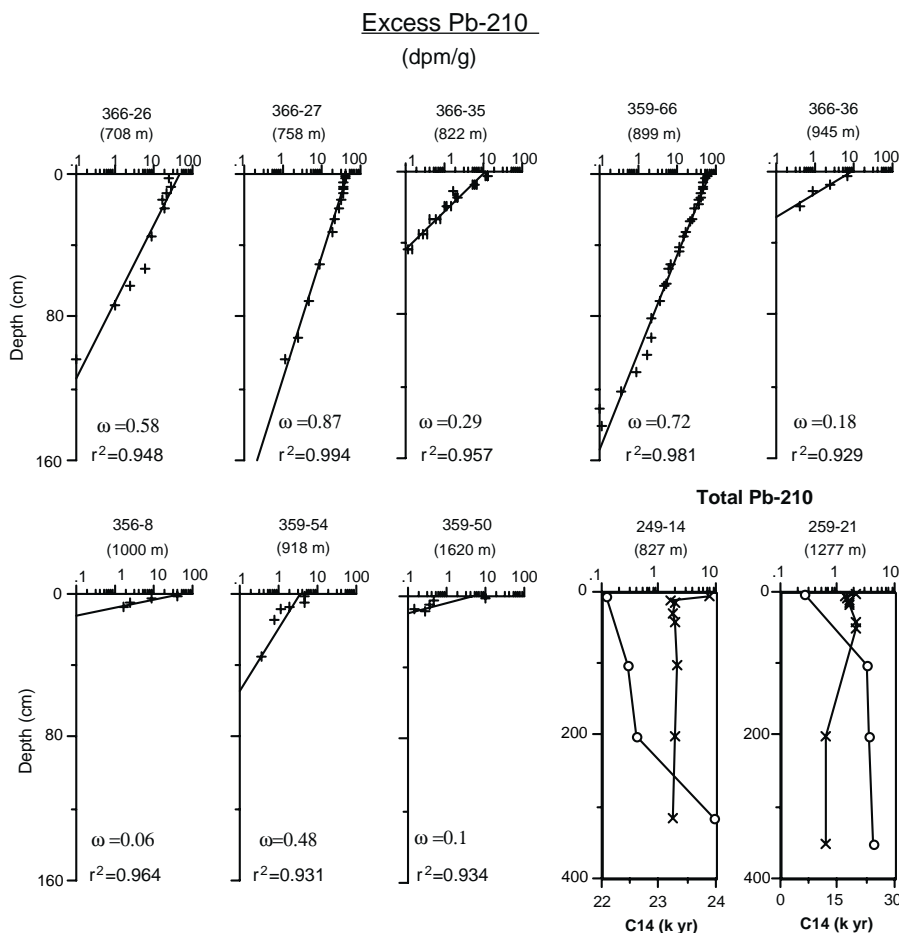


Fig. 7. Excess Pb-210 (+), total Pb-210 (x) and C-14 age (O) profiles, sedimentation rates ( $\omega$ , cm/year), and correlation coefficients ( $r^2$ ).

range 1.2–2.3 dpm/g, resembling the supported Pb-210 values at depth of other stations. This lack of excess Pb-210 indicates an absence of recent sediment accumulation at these stations. In fact, the lack of recent sediment deposition was further demonstrated by the age of the surface sediment organic carbon,  $6032 \pm 69$  (Station 259-21) and  $22,090 \pm 160$  (Station 249-14) years BP, based on the C-14 age measurements (Fig. 7). However, relatively high sedimentation rates were found during the Holocene/Pleistocene at these stations. Sedimentation rates calculated from the C-14 data were 0.37 cm/year (0–200 cm) or 0.11 cm/year (200–350 cm) for Station 249-14, and 0.0057 cm/year (0–100 cm) or 0.13 cm/year (100–310 cm) for Station 259-21.

## 4. Discussion

### 4.1. Rapid sulfate reduction

Integrated sulfate reduction rate varied with overlying water depth in two contrasting patterns. From shelf to slope, integrated sulfate reduction rates decreased with increasing water depth (Fig. 8). However, unusually high sulfate reduction rates were also observed in some sediments at 600–1000 m water depth. Sulfate reduction rates were 2–10-fold higher than values at similar water depths in the study area, and some were even higher than those in the adjacent East China Sea continental shelf sediments (Fig. 8). These unusually high sulfate reduction rates were found in areas where relatively high organic carbon concentrations (%organic carbon  $\leq 0.8\%$ ) were observed west of the Kuroshio. In the region east of the Kuroshio, sulfate reduction rates remained relatively low even though the organic carbon concentrations and the overlying water depths were in a similar range.

As a comparison, sulfate reduction rates from other slope and shelf environments were taken from the literature and were also plotted (Fig. 8). In some slope environments (e.g. Maine, US), sulfate reduction rates decreased rapidly with increasing overlying water depth. Lein (1985) showed that sulfate reduction rates and authigenic

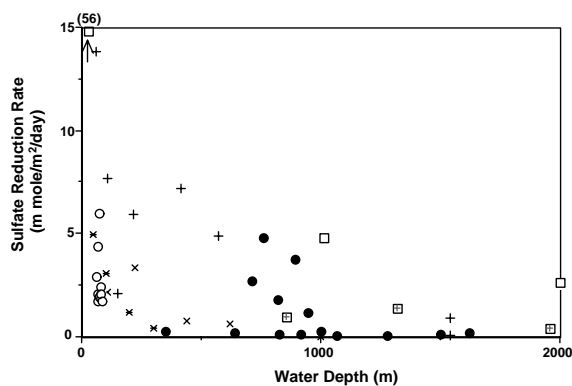


Fig. 8. Integrated sulfate reduction rates in continental shelf and slope sediments. (●): study area; (○): East China Sea (Lin et al., 2000); (◻): Angola and Namibia slope; (+): Gulf of Mexico (Lin and Morse, 1991); (◻): Chile (Thamdrup and Canfield, 1996); (×): Washington, US (Kristensen et al., 1999); (\*): Maine, US (Christensen, 1989).

sulfide burial rates were related to the overlying water depth. Christensen (1989) showed that sulfate reduction rates were an exponential function of the overlying water depth and that sulfate reduction rates decreased 10-fold between 50 and 300 m. Sulfate reduction rates in some of our study areas were higher than those off Maine and Washington, but similar to those observed off Chile. The high sulfate reduction rates we observed in the slope areas showed that sulfate reduction rate is not a simple function of the overlying water depth as observed by Christensen (1989). In fact, Ferdelman et al. (1999) pointed out that high sulfate reduction rates observed in the mid-slope region of the Angola and Namibia region reflected high organic carbon supply from the Benguela upwelling system.

Differences in the regional organic carbon production and deposition may contribute to the observed variations. The slope regions with high sulfate reduction rates were characterized by either a high concentration or a high flux of organic carbon. Thamdrup and Canfield (1996) showed that slope sediments off Chile were characterized by an unusually high concentration of organic carbon produced in the upwelling water. Sackett and Thompson (1963) also showed that the slope of the Gulf of Mexico adjacent to the Mississippi

River received a large amount of terrigenous organic carbon directly from the Mississippi River. High suspended particle concentrations and organic carbon fluxes were also observed in our study area (Sheu et al., 1999; Hung and Chung, 1998). Thus, the high organic carbon flux enhanced sulfate reduction in the slope sediments.

#### 4.2. Sulfate reduction and organic carbon deposition

Organic carbon is one of the primary controlling factors for pyrite formation in marine sediments (Berner, 1970). The continental shelf and major river deltas are the most important environments for the burial of authigenic pyrite (Berner, 1982; Lin and Morse, 1991).

Sulfate reduction rates in deep sea sediments increase with increasing sediment burial rates (Canfield, 1989a, 1991). For comparison, sulfate reduction rates and sediment burial rates of this study are plotted in Fig. 9 together with those of Canfield (1989a). Sulfate reduction rates in the East China Sea continental slope sediments showed a similar positive correlation with sediment burial rates. Sulfate reduction rates and sediment burial rates in the East China Sea continental slope sediments were higher than those

in the deep sea sediments and approached those in the coastal area described by Canfield (1989a). Evidently, the unusually high sedimentation rates observed in the studied slope region played an important role in controlling sulfate reduction.

Sulfate reduction rates ( $r^2 = 0.985$ ) and pyrite-S burial rates ( $r^2 = 0.923$ ) increased linearly with the organic carbon burial rate in the East China Sea slope sediments (Fig. 10). With high sediment burial rate, more organic carbon becomes available to the sulfate reducing bacteria.

The quality of organic carbon was also important in determining the rate of sulfate reduction. The sulfate reduction rate and pyrite sulfide burial rate of the adjacent East China Sea continental shelf were plotted against organic carbon burial rate in Fig. 10. The sulfate reduction rate in both shelf and slope sediments increased linearly with respect to the organic carbon burial rate with different rates of increase (filled and open circles, Fig. 10). The organic carbon burial rates observed in part of the slope region were 2–5-fold higher than those in the shelf region. Consequently, high sulfate reduction and pyrite burial rate were observed in the slope region. However, sulfate reduction rates in the slope region (filled circles) were less than those in the shelf sediments (open circles) given the same organic carbon burial rate (Fig. 10). Evidently, the distance traveled prior to final deposition of the organic carbon on the slope had an effect on organic carbon reactivity.

Decomposition of settling organic matter in the water column of the study area has been inferred by Sheu et al. (1999) from variations in  $\delta C^{13}$  values of the organic carbon in sediment traps. Westrich and Berner (1984) showed that quality as well as concentration of organic matter control sulfate reduction rates in anoxic sediments. Both factors, quality and quantity, are also controlling the observed sulfate reduction rate variations between the shelf and the slope environments of the East China Sea. The organic matter in the shelf region was probably less degraded since it traveled a shorter distance before its deposition. Thus, re-suspension of the organic carbon and re-deposition on the slope may enhance the organic carbon deposition in the slope region

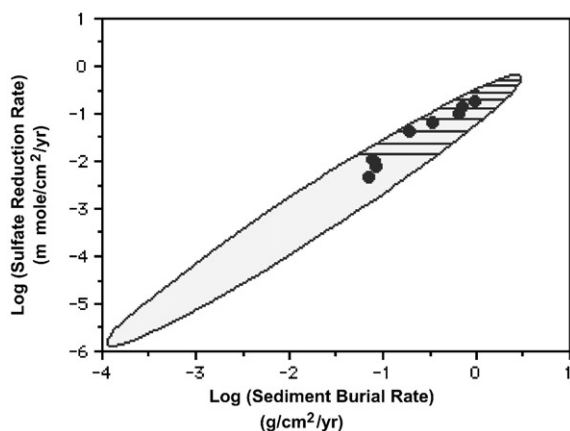


Fig. 9. Integrated sulfate reduction rate varied as a function of sediment burial rate. Filled circles: East China Sea slope data of this study, shaded area and area with horizontal lines: data from Canfield (1989, 1991).

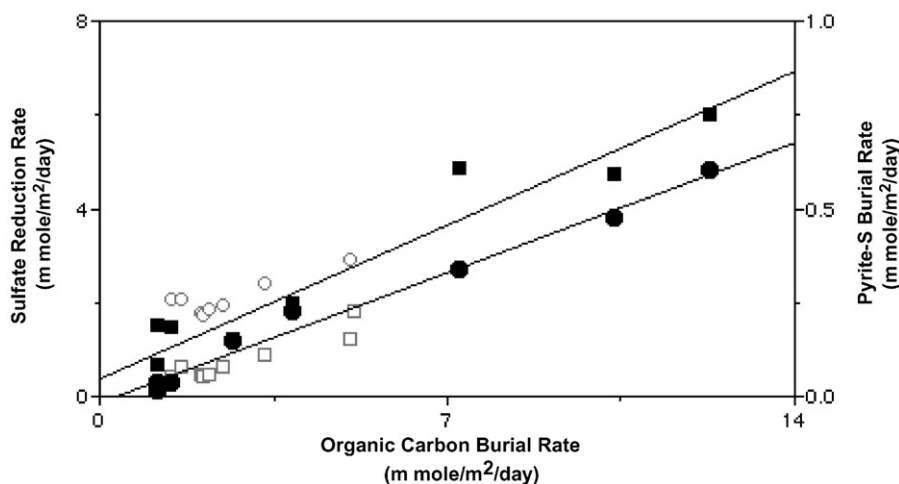


Fig. 10. Integrated sulfate reduction rate (filled and open circles) and pyrite-S burial rate (filled and open squares) as a function of organic carbon burial rate. Filled circles and squares: East China Sea continental slope; open circles and squares: East China Sea continental shelf from Lin et al. (2000). The lines represent linear regression of the sulfate reduction rate and pyrite-S burial rate with respect to the organic carbon burial rate of the slope region. The correlation coefficient ( $r^2$ ) for the sulfate reduction rate vs. organic carbon burial rate is 0.985, and the  $r^2$  for the pyrite-S burial rate vs. organic carbon burial rate is 0.923.

and subsequently increase sulfate reduction rates in the slope sediment with higher organic carbon burial rate.

#### 4.3. Fate of pyrite

Pyrite sulfur was more efficiently buried in the East China Sea slope sediments as compared to the adjacent shelf sediments even though a great percentage of pyrite was re-oxidized prior to its final deposition (Table 1). The supply of organic carbon not only controlled sulfate reduction rates but also controlled the final burial of pyrite. The rate of pyrite sulfur burial increased with increasing organic carbon burial rate in the slope sediments (filled squares, Fig. 10) as well as in the shelf sediments (open squares). Similar to the C/S ratio showing that the concentration of organic carbon limits pyrite formation in the normal marine environment (Bernier, 1970, 1982; Goldhaber and Kaplan, 1974; Raiswell and Bernier, 1985; Lin and Morse, 1991), the observed linear relationships between organic carbon and pyrite sulfur or sulfate reduction, showed that organic carbon deposition is the primary controlling factor for pyrite formation in the studied slope

environments. Notice that pyrite sulfur burial rates and pyrite concentrations in part of the slope region were unusually high.

Most of the sulfide was re-oxidized before its final burial in sediments. However, the fractions of pyrite re-oxidized in some of the slope area are higher than that of the adjacent East China Sea continental shelf sediments. The concentrations of pyrite sulfur and pyrite sulfur burial rates are higher in the East China Sea slope sediments than those in the shelf sediments even though sulfate reduction rates are similar (see Figs. 5, 8 and 10). The relatively high efficiency of pyrite preservation as well as the higher sulfate reduction rates observed in the East China Sea slope environment demonstrated that sedimentation rate indeed plays a pivotal role in determining the fate of pyrite in the studied slope sediments. As a result of higher pyrite sulfur burial rate and sulfate reduction rate, the southern East China Sea continental slope environment is an efficient pyrite sulfur burial environment. The results indicate that the slope environment could be an even more important sulfide burial environment in case more organic carbon should become available.

Table 1

Sedimentation rates, sulfate reduction rates, organic carbon and Pyrite-S burial rates, %Pyrite re-oxidation rates and water depth at the studied stations

Station number	Water depth (m)	Sedimentation rate (cm/year)	Sulfate reduction rate (mmol/m <sup>2</sup> /day)	Org. carbon burial rate <sup>a</sup> (mmol/m <sup>2</sup> /day)	Pyrite-S burial rate <sup>a</sup> (mmol/m <sup>2</sup> /day)	%Pyrite re-oxidation <sup>b</sup>
366-26	708	0.58	2.710	7.25	0.606	22
366-27	758	0.87	4.810	12.27	0.752	16
366-35	822	0.29	1.810	3.87	0.248	14
366-36	945	0.18	1.198	2.69	0.156	13
359-66	889	0.72	3.800	10.35	0.593	16
359-50	1620	0.10	0.214	1.19	0.025	12
356-8	1000	0.06	0.287	1.16	0.189	66
356-27B	1498	0.08	0.132	1.17	0.087	66
359-54	918	0.10	0.279	1.46	0.185	66
366-24	350	—	0.637	—	—	—
366-11	637	—	0.330	—	—	—
366-33	734	—	2.710	—	—	—
249-14	827	—	0.220	—	—	—
356-18	1068	—	0.095	—	—	—
259-21	1277	—	0.162	—	—	—

<sup>a</sup> Organic carbon and pyrite-S burial rate:  $J_z = \rho(1 - \phi)\omega[C]$ , where  $J_z$  is flux of carbon or pyrite across a sediment horizon at depth  $z$  ( $z = 100$  cm);  $\rho$  = dry bulk density;  $\phi$  = porosity;  $\omega$  = sedimentation rate;  $[C]$  = organic carbon or pyrite-S concentrations.

<sup>b</sup> %Pyrite re-oxidation =  $100 \times [1 - (\text{pyrite-S burial rate/sulfate reduction rate})]$ .

—: Sedimentation rate could not resolve by the Pb-210 method.

## Acknowledgements

The authors thank Dr. Neil Suits, two anonymous reviewers and Dr. Michael Bacon for their constructive suggestions. We wish to thank captain and crew of the R/V *Ocean Researcher-I* for their assistance in sample collection and D. Chambers of the Rafter Radiocarbon Laboratory, New Zealand, for the C-14 measurements. This research was supported, in part, by grant from the ROC National Science Council.

## References

- Berner, R.A., 1970. Sedimentary pyrite formation. *American Journal of Science* 268, 1–23.
- Berner, R.A., 1982. Burial of organic carbon and pyrite sulfur in the modern ocean: its geochemical and environmental significance. *American Journal of Science* 282, 451–473.
- Berner, R.A., 1987. Models for carbon and sulfur cycles and atmospheric oxygen: application to Paleozoic geologic history. *American Journal of Science* 287, 177–196.
- Berner, R.A., 1998. The sulfur cycle and atmospheric oxygen. *Science* 282, 1426–1427.
- Berner, R.A., Canfield, D., 1989. A new model for atmospheric oxygen over Phanerozoic time. *American Journal of Science* 289, 333–361.
- Berner, R.A., Petsch, S.T., Lake, J.A., Beerling, D.J., Popp, B.N., Lane, R.S., Laws, E.A., Westley, M.B., Cassar, N., Woodward, F.I., Quick, W.P., 2000. Isotope fractionation and atmospheric oxygen: implications for Phanerozoic O<sub>2</sub> evolution. *Science* 287, 1630–1633.
- Canfield, D.E., 1989a. Sulfate reduction and oxic respiration in marine sediments: implications for organic carbon preservation in euxinic environments. *Deep-Sea Research I* 36, 121–138.
- Canfield, D.E., 1989b. Reactive iron in marine sediments. *Geochimica et Cosmochimica Acta* 53, 619–632.
- Canfield, D.E., 1991. Sulfate reduction in deep-sea sediments. *American Journal of Science* 291, 177–188.
- Canfield, D.E., 1993. Organic matter oxidation in marine sediments. In: Wollast, R., et al. (Ed.), *Interaction of C, N, P and S Biogeochemical Cycles*. Springer, Berlin, pp. 333–363.
- Canfield, D.E., 1998. A new model for Proterozoic ocean chemistry. *Nature* 396, 450–453.
- Canfield, D.E., Raiswell, R., Westrich, J.T., Reaves, C.M., Berner, R.A., 1986. The use of chromium reduction in the analysis of reduced inorganic sulfur in sediments and shales. *Chemical Geology* 54, 149–155.

- Christensen, J.P., 1989. Sulfate reduction and carbon oxidation rates in continental shelf sediments, an examination of offshelf carbon transport. *Continental Shelf Research* 9, 223–246.
- Chung, Y., Chang, W.C., 1995. Pb-210 fluxes and sedimentation rates on the lower continental slope between Taiwan and the South Okinawa Trough. *Continental Shelf Research* 15, 149–164.
- Cline, J.D., 1969. Spectrophotometric determination of hydrogen sulfide in natural waters. *Limnology and Oceanography* 14, 454–458.
- Cornwell, J.C., Morse, J.W., 1987. The characterization of iron sulfide minerals in marine sediments. *Marine Chemistry* 22, 193–206.
- Ferdelman, T.G., Fossing, H., Nermann, K., 1999. Sulfate reduction in surface sediments of the southeast Atlantic continental margin between 15°38'S and 27°57'S (Angola and Namibia). *Limnology and Oceanography* 44, 650–661.
- Flynn, W.W., 1968. The determination of low levels of Polonium-210 in environmental materials. *Analytica Chimica Acta* 43, 221–227.
- Folk, R.L., 1968. *Petrology of Sedimentary Rocks*. Hemphills, Austin, TX, 170pp.
- Garrels, R.M., Lerman, A., 1984. Coupling of the sedimentary sulfur and carbon cycles—an improved model. *American Journal of Science* 284, 989–1007.
- Goldhaber, M.B., Kaplan, I.R., 1974. The sulfur cycle. In: Goldberg, E.D. (Ed.), *The Sea*, Vol. 5. Wiley, New York, pp. 569–655.
- Gong, G.-C., Shiah, F.-K., Liu, K.-K., Wen, Y.-H., Liang, M.-H., 2000. Spatial and temporal variation of chlorophyll *a*, primary productivity and chemical hydrography in the southern East China Sea. *Continental Shelf Research* 20, 411–436.
- Holland, H.D., 1978. *The Chemistry of the Atmosphere and Oceans*. Wiley, New York, 351pp.
- Huang, K.-M., Lin, S., 1995. The carbon-sulfide-iron relationship and sulfate reduction rate in the East China Sea continental shelf sediments. *Geochemical Journal* 29, 301–315.
- Hung, G.-W., Chung, Y.-C., 1998. Particulate fluxes, 210Pb and 210Po measured from sediment trap samples in a canyon off northeastern Taiwan. *Continental Shelf Research* 18, 1475–1491.
- Jorgensen, B.B., 1978. A comparison of methods for the quantification of bacterial sulfate reduction in coastal marine sediments. I. Measurement with radiotracer techniques. *Geomicrobiology Journal* 1, 29–47.
- Jorgensen, B.B., 1982. Mineralization of organic matter in the sea bed—the role of sulfate reduction. *Nature* 296, 643–645.
- Kristensen, E., Devol, A.H., Hartnett, H.E., 1999. Organic matter diagenesis in sediments on the continental shelf and slope of the Eastern Tropical and temperate North Pacific. *Continental Shelf Research* 19, 1331–1351.
- Lasaga, A.C., 1989. A new approach to isotopic modeling of the variation of atmospheric oxygen through the Phanerozoic. *American Journal of Science* 289, 411–435.
- Lein, A.Y., 1985. The isotopic mass balance of sulfur in oceanic sediments (the Pacific Ocean as an example). *Marine Chemistry* 16, 249–257.
- Lin, S., Morse, J.W., 1991. Sulfate reduction and iron sulfide mineral formation in Gulf of Mexico anoxic sediments. *American Journal of Science* 291, 55–89.
- Lin, S., Liu, K.K., Chen, M.P., Chang, F.Y., 1992. Distribution of organic carbon in the KEEP area continental margin sediments. *Terrestrial, Atmospheric, Oceanic Science* 3, 365–378.
- Lin, S., Huang, K.-M., Chen, S.-K., 2000. Organic carbon deposition and its control on iron sulfide formation of the southern East China Sea continental shelf sediments. *Continental Shelf Research* 20, 619–635.
- Lin, S., Hsieh, I.-J., Huang, K.-M., Wang, C.-H., 2002. Influence of the Yangtze River and grain size on the spatial variations of heavy metals and organic carbon in the East China Sea continental shelf sediments. *Chemical Geology* 182, 377–394.
- Liu, K.-K., Gong, G.-C., Lin, S., Shyu, C.-Z., Yang, C.-Y., Wei, C.-L., Pai, S.-C., Wu, C.-K., 1992. The year-round upwelling at the shelf break near the northern tip of Taiwan as evidenced by chemical hydrography. *Terrestrial, Atmospheric and Oceanic Sciences* 3, 234–276.
- Narita, H., Harada, K., Tsunogai, S., 1990. Lateral transport of sediment particles in the Okinawa Trough determined by natural radionuclides. *Geochemical Journal* 24, 207–216.
- Nittrouer, C.A., Sternberg, R.W., Carpenter, R., Bennett, J.T., 1979. The use of Pb-210 geochronology as a sedimentological tool: application to the Washington continental shelf. *Marine Geology* 31, 297–316.
- O'Dell, J.W., Pfaff, J.D., Gales, M.E., McKee, G.D., 1984. The determination of inorganic anions in water by ion Chromatography. Method 300.0, US EPA 600/4.84.017, 5pp.
- Raiswell, R., Berner, R.A., 1985. Pyrite formation in euxinic and semi-euxinic sediments. *American Journal of Science* 285, 710–724.
- Sackett, W.M., Thompson, R.R., 1963. Isotopic organic carbon composition of recent continental derived clastic sediments of eastern gulf coast, Gulf of Mexico. *Bulletin American Association of Petroleum Geologists* 47, 525–538.
- Sheu, D.-D., Jou, W.-C., Chung, Y.-C., Tang, T.-Y., Hung, J.-J., 1999. Geochemical and carbon isotopic characterization of particles collected in sediment traps from the East China Sea continental slope and the Okinawa Trough northeast of Taiwan. *Continental Shelf Research* 19, 183–203.
- Shiah, F.-K., Gong, G.-C., Liu, K.-K., 1995. A preliminary survey on primary productivity measured by the <sup>14</sup>C assimilation method in the KEEP area. *Acta Oceanographica Taiwanica* 34, 1–15.
- Shokes, R.K., 1976. Rate dependent distributions of Lead-210 and interstitial sulfate in sediments of the Mississippi River Delta. Ph.D. Thesis, Texas A&M University, 122pp.
- Smith, J.D., Hamilton, T.F., 1984. Improved technique for recovery and measurement of polonium-210 from environmental materials. *Analytica Chimica Acta* 160, 69–77.

- Stuiver, M., Polach, H.A., 1977. Reporting of  $^{14}\text{C}$  data. *Radiocarbon* 19, 355–363.
- Suits, N.S., Arthur, M.A., 2000. Sulfur diagenesis and partitioning in Holocene Peru shelf and upper slope sediments. *Chemical Geology* 163, 219–234.
- Tang, T-Y., Tai, J.-H., Yang, Y.-J., 2000. The flow pattern north of Taiwan and the migration of the Kuroshio. *Continental Shelf Research* 20, 349–371.
- Thamdrup, B., Canfield, D.E., 1996. Pathways of carbon oxidation in continental margin sediments off central Chile. *Limnology and Oceanography* 41, 1629–1650.
- Volkov, I.I., Rozanov, A., 1983. The sulfur cycle in oceans. Pt. I, Reservoirs and fluxes. In: Ivanov, M.V., Freney, J.R. (Eds.), *The Global Biogeochemical Sulfur Cycles*, SCOPE 19. Wiley, New York, pp. 357–423.
- Westrich, J.T., Berner, R.A., 1984. The role of sedimentary organic matter in bacterial sulfate reduction: the G model tested. *Limnology and Oceanography* 29, 236–249.